Theoretical and Applied Climatology (2020) 141:31–41
https://doi.org/10.1007/s00704-020-03158-8

ORIGINAL PAPER

Cooling effects of different wetlands in semi-arid rural region of Northeast China

Zhang Wenguang[1] · Wang Wenjuan[1] · Hou Guanglei[1] · Gong Chao[1] · Jiang Ming[1] · Lyu Xianguo[1]

Received: 7 December 2019 / Accepted: 18 February 2020 / Published online: 21 March 2020

Abstract

Wetland ecosystems play an important role in regulating local and regional climates through evaporative cooling effects that affect the exchange of energy and water with atmosphere. A lot of researches had been focused on the wetland cooling effect, especially in mitigating urban heat island effect. However, the intensity and influencing factors of wetland cooling effect currently cannot be thorough explained. In this study, we assessed the cooling effect of wetlands with different types in rural area of Northeast China by using split-window algorithm (SWA) to estimate land surface temperatures (LST) from Landsat-8 thermal infrared sensor. We used correlation analysis to examine the relationships between characteristics of wetlands and cooling effect. Our results showed that paddy fields had the largest cooling effects than lakes followed by marshes for human disturbance. Size and shaped complexity were important characteristics to determine wetland cooling effects. Although our results suggested that larger size of wetlands might have higher intensity and spatial extent of cooling effects, small size of wetlands might have large or almost similar amount of cooling effects with the larger ones. Our findings have important implications for land managers and policy makers to design effective plans for conservation and climate change adaptation.

1 Introduction

Climate change has profound impacts on distribution, structure, and function of wetland ecosystems (Burkett and Kulser 2000; Lahmer et al. 2001; Fu and Li 2001). On the contrary, wetland ecosystems play an important role in regulating local and regional climates through the exchange of energy and water with atmosphere (Mitsch and Gosselink 2007; Gerhard 2003; Gong et al. 2011). For example, lake wetland can increase atmospheric humidity, reduce the daily maximum temperature, and increase the daily minimum temperature in summer (Hostetler et al. 1993; Gordon 1995). Meanwhile, the composition, structure, and distribution of wetland landscape also are correlated to climatic factors (Burkett and Kulser 2000; Fu and Li 2001). And the impact scale includes global, regional, and local for the wetlands with different albedo, heat capacity, and roughness (Turner et al. 2000; Lahmer et al. 2001). In recent years, a lot of researches focused on the cooling effect of wetland or water body in urban landscape and concluded that the water body or wetlands play an important role in reducing heat islands effects and regulating microclimate (Ranhao et al. 2012; Zhang et al. 2016; Du et al. 2016; Wang et al. 2017; Zhenshan et al. 2019). However, the intensity and influencing factors of wetland cooling effect currently are not thoroughly explained.

Over the past decades, wetland ecosystems have been intensively degraded globally both in distribution and diversity (Ramsar Convention on Wetlands, FAO, International Water Management Institute 2014), and more than 50% of wetlands have been replaced by agricultural uses since the 1900s AD (Davidson 2014; Ramsar Convention on Wetlands FAO 2014). As a result, the climate regulating services of wetland are diminished (Costanza et al. 1998; Chen and Lu 2003; Li et al. 2018). Especially, inland wetlands (e.g., marsh, lakes, and ponds) that are usually small and isolated, provide a range of ecological services (Costanza et al. 1997; Gao et al. 2002; Gao et al. 2003; Gerhard 2003; Nie and Wang 2010). For it is technically and financially feasible to create or modify, the inland wetlands play a central role in local and regional wetland management and restoration activities that aim to mitigate and adapt to climate change (Çağdaş and Halime 2018). However, different types of wetlands may have different intensity and spatial extent of cooling effects for different

✉ Zhang Wenguang
zhangwenguang@iga.ac.cn; zhangwenguang@iga.ac.cn

[1] Key Laboratory of Wetland Ecology and Environment, Northeast Institute of Geography and Agroecology (IGA), Chinese Academy of Sciences (CAS), Changchun 130102, People's Republic of China

biophysical properties and characteristics (Bai et al. 2013; Gou et al. 2014; Zhang et al. 2014). Hence, understanding the cooling effects of different wetland types and their important characteristics is essential for land managers and policy makers to design effective plans for conservation and climate change adaptation.

Here, we provide an assessment of the cooling effects of different wetland types on local climates in a semi-arid region of Northeast China. Northeast China has the largest area of wetlands in China including marshes, lakes, and paddy fields (Mingquan et al. 2008). Since the mid-1980s, a large number of wetlands have been converted to other land uses primarily agricultural lands due to a rapid growing population of China (Li et al. 2016). As a result, over the past decades, natural wetlands have been rapidly shrinking, concurrently farmland and other land use have been dramatically expanding. Specifically we addressed (1) how do the cooling effects vary among different wetland types (e.g., lakes, marshes, and paddy fields)? and (2) which factors influence cooling effects by natural wetland characteristics or human interference?

2 Data and methods

2.1 Study area

The study area (43°57′-46°46′N, 121°38′-126°22′E) covers 4.69 million hectares and is located in the western part of Jilin province, Northeast China (Fig. 1a). It is a low alluvial plain, in which digital elevation models (DEMs) values for most of the area range from 100 to 200 m (Fig. 1b). The area is a transitional zone from semi-arid climate to sub-humid climate with mean annual precipitation and evaporation of about 400 mm, 1600–2000 mm, respectively. Average temperature has been increased by 1.5°C and average precipitation has been reduced by 60 mm over the past 38 years, which are dramatically higher than the global average (Chen et al. 2011; Shen et al. 2014).

Regulating the microclimate is the main ecosystem service of wetland. And the change of land-use type will alter the quantity and spatial distribution of wetlands, consequently, may influence the local climate (Li et al. 2018). Thus, the wetland is a more important land-cover type in influencing ecological environment in the study area than other areas (Wang et al. 2008) (Fig. 1).

2.2 Method and materials

2.2.1 Land cover

We used Landsat 8 images (30 × 30 m) and eCognition software to conduct atmospheric correction, geometric correction, and image fusion and extract land cover types. In the remote sensing classification, the decision tree analysis was used by combining the manual and automatic methods. The manual method was used for the types with clear spectral division, and the automatic method (nearest neighbor method) was used for the types with large spectral changes and unclear rules. Land cover classification method (LCCs) developed by Food and Agriculture Organization of the United Nations (FAO) and the ecosystem classification system developed by the Ministry of environmental protection of the People's Republic of China was combined. We included seven major land cover types including artificial surfaces of human activities (e.g., residence, construction, and extraction), forests, water bodies (e.g., river, lake, reservoir, and pond), marshes, agricultural lands (primarily paddy fields), grasslands, and others (e.g., saline-alkaline and sands). The overall accuracy of the land cover classification was 93.54% with an overall Kappa coefficient of 0.92, indicating accurate classification.

2.2.2 Land surface temperature

In this study, we used Landsat-8 thermal infrared sensor (TIRS) with two thermal infrared spectral bands to retrieve land surface temperatures (LST). Cloud-free images were delivered by the Geospatial Data Cloud (http://www.gscloud.cn/), acquired at

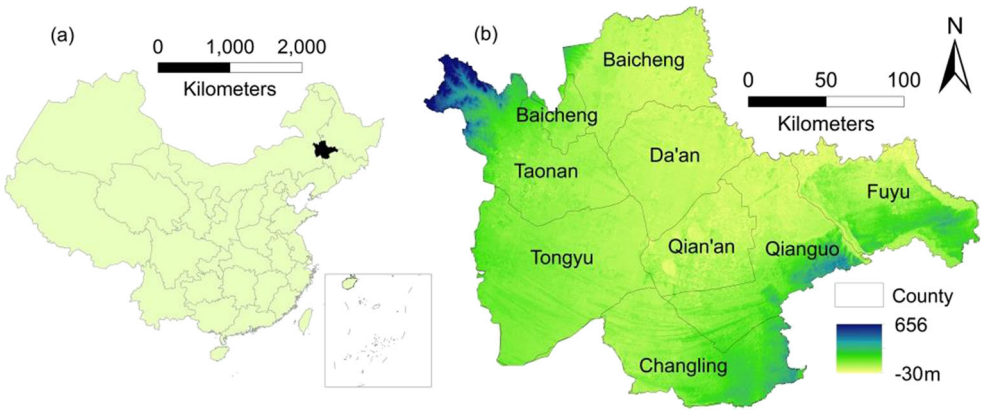

Fig. 1 The study area included geographic location in China (**a**) and counties and digital elevation models (DEMs) (**b**)

approximately 11:00 a.m. (Beijing time) on 1 August 2015. Before LST estimation, the two Landsat-8 OLI/TIRS images were radiometrically calibrated and geometrically corrected with an accuracy of fewer than 0.5 pixels. All image preprocessing was performed in the ENVI 5.1 software.

The split-window algorithm (SWA) removes the atmospheric effect through differential atmospheric absorption in the two adjacent thermal infrared channels centered at about 11 and 12 μm, and the linear or nonlinear combination of the brightness temperatures is finally applied for LST estimation (Offer et al. 2014, Du et al. 2015). So in this paper, we used split-window algorithm to estimate land surface temperature (LST) from Thermal Infrared Sensor (TIRS) aboard Landsat 8. The SWA is derived from a first-order Taylor-series linearization of the radiative transfer equation (Yu et al. 2007) and its formulation takes the general form (Qin et al., 2001a).

$$T_s = A_0 + A_1\ T_{10} - A_2\ T_{11} \quad (1)$$

where T_s is LST and T_{10} and T_{11} are the brightness temperature of the two thermal infrared bands 10 and 11 of Landsat-8. A_0, A_1, and A_2 are coefficients which had been calculated using the formula of Qin et al. (2001b) or Zhenshan et al. (2019). Equation (1) used three parameters, namely brightness temperature, land surface emissivity, and atmospheric transmittance.

The brightness temperature by the header file of Landsat 8. The DN values of the image are converted radiance using gain and bias values (Qin and Gao 2006).

$$RD = gain^{*}\ DN + bias \quad (2)$$

where RD is the radiance of the cell value and gain and bias are values for a specific band in header file. Then the radiance converted brightness temperature without atmospheric correction.

$$T = \frac{K_2}{\ln\left(\frac{K_1}{RD_i} + 1\right)} \quad (3)$$

where T is the brightness temperature and K_1 and K_2 are constants. RD_i is the radiance of the band 10 and 11 of Landsat 8.

For land surface emissivity, the procedures for emissivity estimation form the infrared and visible band are discussed in detail elsewhere (Snyder, Wan et al. 1998, Dash et al. 2002, Li et al. 2013; Zhenshan et al. 2019). In this research, we also adapted the procedures using Landsat 8 OLI to indirectly estimate the land surface emissivity in TIRS band.

Based on the Modtran 4.0 simulation, the relation between water vapor and atmospheric transmittance was conducted in mid-latitude summer and 1976 standard US atmospheric profile (see Table 1) (Qin 2005). Considering that the MODIS have the same time passing the study area with Landsat 8, the MOD7 in 1 August 2015 was downloaded to obtain data for the water vapor. Then the atmospheric transmittance was calculated using the mid-latitude summer formula shown in Table 1.

2.3 Quantifying the cooling effects of wetlands

We chose the four most representative wetland types to investigate the cooling effects including marsh, lake, mixed lake and marsh (MLM), and paddy fields (as artificial wetland). In this study, a total of 206 wetlands were selected to study wetland cooling effects, including 95 lakes, 71 marshes, 18 MLMs, and 22 paddy fields. In order to estimate cooling effect of wetland, the wetland scope, including water and vegetation ratio, was digitalized from the google earth map. We built 40 buffers with the distance of 50 m from edge of every wetland, and the buffers distance is total 2000 m. Then we overlaid the layer of buffer and the LST images, and statistics out the mean LST for every buffer. We profiled the mean LST of buffers to search the edge of the cooling effect. We defined the value which was first equal or greater than the subsequent value of the mean LST profile from inside buffer out, as "edge temperature" of the cooling effect (Ranhao et al. 2012). We then calculated the temperature difference in LST for each buffer (*Diff_LST*) between the wetland and given buffer (Eq. 4). We identified the maximum cooling buffer (k) for each wetland (Eq. 5), in which *Diff_LST* decreased sharply or reached a relatively flat level. Since LST around a wetland may be influenced by other wetlands or different land use, we chose the first decreased buffer to measure the maximum cooling distance of each wetland (*Max Distance*). We quantified the cooling intensity for each wetland using temperature gradient (*Temp_gradient*) which was calculated as the ratio between temperature difference at the maximum cooling buffer and the maximum cooling distance (Eq. 6). We also averaged the maximum cooling distance and temperature gradient for four wetland types to represent an average response across the region.

$$Diff\_LST_{(i,j,n)} = LST_{(i,j,n)} - LST_{(i,j,0)} \quad (4)$$

$$Max\ Distance_{(i,j)} = 50 \times k \quad (5)$$

$$Temp\_grdient_{(i,j)} = \frac{Diff\_LST_{(i,j,k)}}{MaxDistance_{(i,j)}} \quad (6)$$

where i was the wetland type (1, 2, 3, 4), j was one of the wetland j (1, 2… 95/71/18 or 22) for wetland type i, n was the one of the buffer for the wetland type i and wetland j, and k

Table 1 Relationship between atmospheric transmittance and water vapor

Profile	Estimation equation	R^2
1976 US standard	$\tau_{10} = -0.1146w + 1.0286$	0.9882
	$\tau_{11} = -0.1568w + 1.0083$	0.9947
Mid-latitude summer	$\tau_{10} = -0.1134w + 1.0335$	0.986
	$\tau_{11} = -0.1546w + 1.0078$	0.996

was the maximum cooling buffer for the wetland type *i* and wetland *j*.

We compared the cooling effects in terms of maximum cooling distance and temperature gradient among different wetland types using Welch's *t* test that is usually used for unequal sample size. We used spearman rank correlation coefficient to investigate the relationship between cooling effects and wetland area and landscape shape index (LSI), which quantified the size and shape complexity of wetlands, respectively. Since we did not exclude the outliers (e.g., very large lakes or paddy fields), we presented the median values (e.g., area, LSI, maximum cooling distance, and temperature gradient).

In order to investigate the daily dynamics of cooling effects of wetlands, we chose the Niuxintaobao marsh and Zhangjialu Lake as examples to monitor the daily climatic variables including air temperature and relative humidity of inner and outside (100 m) of wetlands using HOBO series temperature and humidity recorder (Pro V2). For synthetic evaluation of cooling effect, we also measured the water depth of wetlands by sounding rod method.

3 Results

3.1 Wetland characteristics

In terms of the spatial distribution of land cover type, the land cover type with the widest spatial distribution in the region is farmland, with total area about 30,556.45 km^2, and the second land cover is grass with 6208.15 km^2. The total area of wetlands was 4305.85 km^2, about 9.18% of the area. Most rivers have been cut off due to natural and human causes. The artificial surface area increased to 2018.48 km^2, and the residential area continued to expand, mainly distributed among the dry land landscape (Fig. 2).

Our study area was mainly composed of farmland and grasslands at year 2015, which accounted for 65% and 13% of the whole region (Fig. 2). The farmland increased by 20% compared with the historical records at year 1954 largely at the expense of grasslands and marshes. The random spatial distribution of wetlands that we focused in this study including water bodies, marshes, MLMs, and paddy fields were shown in Fig. 3 a and the LST were shown in Fig. 3 b with the different temperature ranged from 15.2 to 44.3 °C.

The median area of lakes, marshes, MLMs, and paddy fields averaged 74 ha, 95 ha, 171 ha, 24 ha, respectively (Fig. 4a). Most of lakes were within 300 ha with several large lakes of over 1000 ha (Chagan Lake, Dabushu Lake, and Yueliangpao Lake). The median LSI was largest for marshes (2.84), followed by paddy fields (1.36), MLM (1.24), and lakes (1.17) indicating relatively greater shape complexity for marsh (Fig. 4b).

The median surface temperature varied significantly among lakes, marshes, MLMs, and paddy fields ($p < 0.05$), with the lowest surface temperature for paddy fields (26.89 °C) followed by lakes (27.57 °C), MLMs (29.77 °C), and marshes (29.96 °C) (Fig. 4c).

3.2 Wetland cooling effects

The maximum cooling distance ($p < 0.05$) and the temperature gradient ($p < 0.05$) were significantly different among four wetland types (Fig. 5). The median maximum cooling distance was longest for paddy fields (350 m) followed by lakes (300 m), MLMs (270 m), and marshes (250 m) (Fig. 5a).The median temperature gradient averaged 8.15 °C/km, 8.08 °C/km, 5.72 °C/km, and 5.01 °C/km for paddy fields, lakes, MLMs, and marshes, respectively (Fig. 5b).

For four wetland types, the maximum cooling distance and temperature gradient were marginally positively related to wetland area. The cooling distances of lake ranged from 100 to 750 m and had positive correlation with area, temperature difference, and temperature gradient with correlation coefficient 0.507($p < 0.01$), 0.685 ($p < 0.01$), and 0.254 ($p < 0.05$), respectively. The temperature gradient was positively correlated to area with a Spearman Rho of 0.433 ($p < 0.01$). And the LSI index is negatively correlated with cooling distance and temperature gradient with correlation coefficient 0.205 ($p < 0.05$) and 0.248 ($p < 0.05$), respectively.

The area of marsh ranged from 102.68 to 1770.78 ha with the main plant species of *Phragmites communis*, *Scirpus triqueter*, *Typha orientalis Presl*, etc. The LSI was significantly negatively correlated with area with coefficient of about 0.602 ($p < 0.01$) indicating that the topography in west Jinlin Province was relatively flat and the marsh distributed randomly in it. And the temperature gradient firstly increase and then decrease with the increase of area (Fig. 6). When the area of marsh reached about 7–10 km^2, the temperature gradient was at its maximum value. The cooling distance of marsh showed positive correlation to temperature difference with correlation coefficient about 0.592 ($p < 0.01$).

The MLM had the characteristics of lakes and marsh, except a little small patches, and most of MLM were more than 100 ha for the flat terrain. The average proportion of water was about 0.66, with a range from 0.99 to 0.01. The cooling distances ranged from 100 to 1000 m, same with the marshes. The temperature difference ranged from 0.02 to 6.32 °C. Cooling distance of MLM positively correlated with area and temperature difference with the coefficient of about 0.678 ($p < 0.01$) and 0.534 ($p < 0.05$), respectively.

In the study, the area of paddy field ranged from 3.43 to 261.48 ha, and the cooling distances ranged from 150 to 1200 m, more than other wetland types. The mean temperature difference was 2.74 °C, ranging from 0.14 to 6.14 °C. The

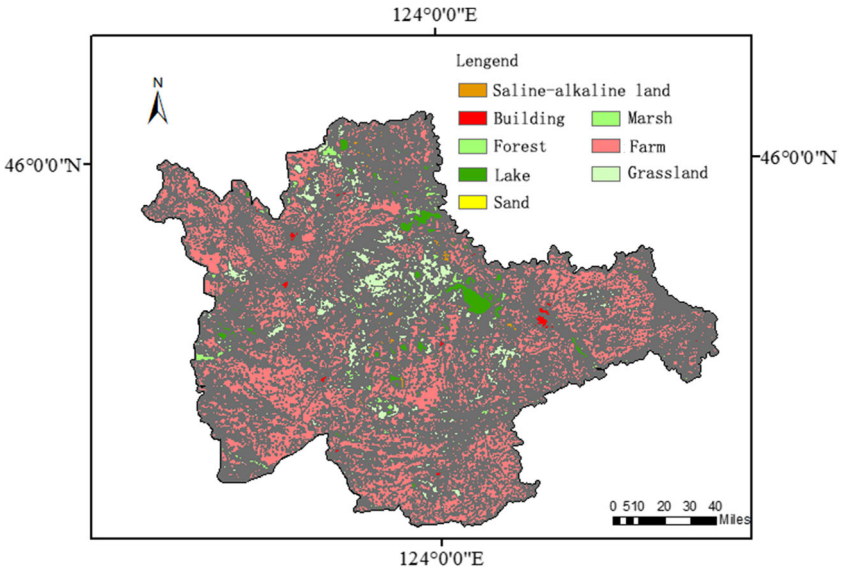

Fig. 2 Major land cover types at year 2015 for our study area that were derived from the Landsat 8 images

cooling effect was obvious for the surround land use mostly was bare or saline and alkaline land with higher LST.

3.3 The tendency of cooling effect

The four wetland types have showed different tendency. The area of lake has logarithmic correlation with cooling distance and temperature difference, and the coefficients were 0.273 ($p < 0.01$) and 0.252 ($p < 0.01$). The curve showed that the cooling distance and temperature difference increased dramatically when the area was less than 2 km^2, then into slow growth stage when the area was between 2 and 10 km^2. When the lake area was more than 10 km^2, the cooling distance and temperature difference did not increase a lot (Fig. 7a).

The cooling distance and temperature difference of marsh both showed the same quadratic polynomial relationship with the wetland area. The cooling affect also showed the same results with Fig. 6, but the correlation coefficient was rather small (Fig. 7b).

The area of MLM showed quadratic polynomial relationship with turning distance and temperature difference, with coefficient of about 0.487 ($p < 0.01$) and 0.228 ($p < 0.01$). The cooling distance and temperature difference increased with the area expansion (Fig. 7c).

The relationship of artificial wetland was relatively complex. The cooling distance had significant linear relationship with the area, and the temperature difference showed logarithmic correlation with the area. When the artificial wetland area was greater than 0.5 km^2, the temperature difference did not change a lot (Fig. 7d).

From the analysis of the study, it was also important to note that a large number of wetlands with small area had long maximum cooling distance and temperature distance especially for lakes, marshes, and paddy fields.

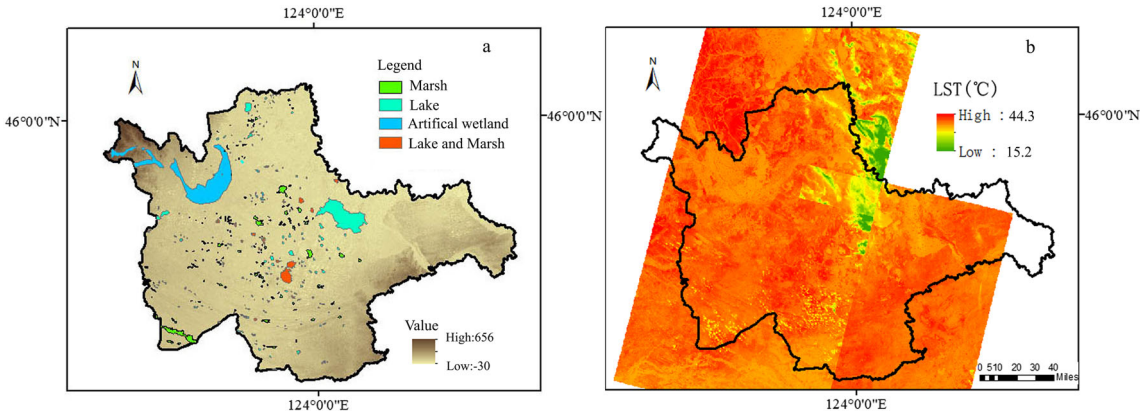

Fig. 3 The selected wetlands (**a**) and land surface temperature (LST°C) (**b**)at 11:00 a.m. on August 1, 2015 for our study area derived from the Landsat 8 images. The selected wetlands included water bodies, marshes, mixed lake and marsh (MLM), and paddy fields

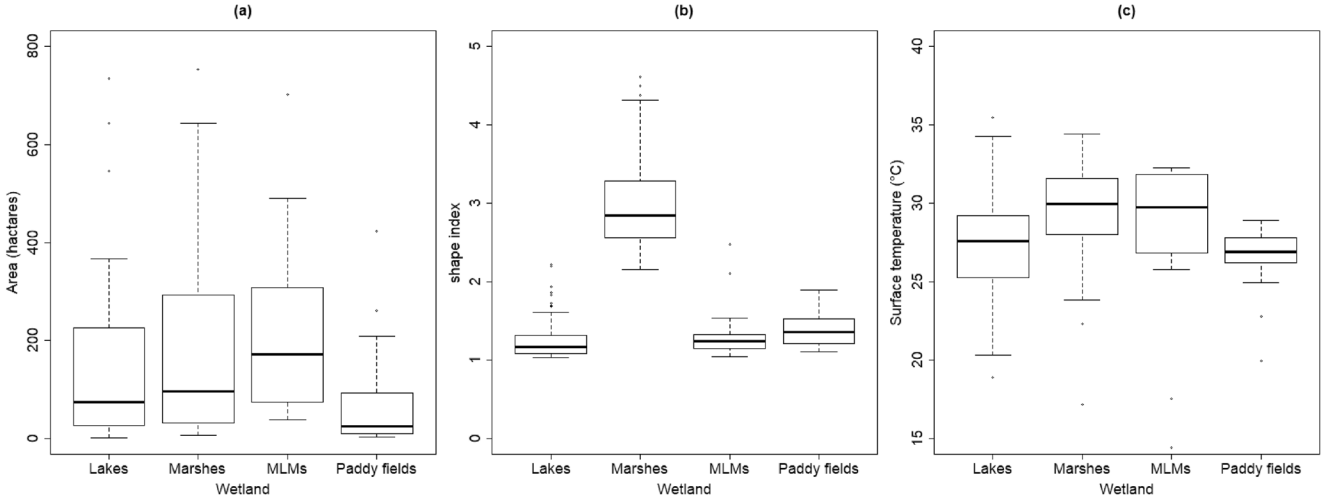

Fig. 4 The characteristics of different types of wetlands in the west of Jinlin province. **a** The area range and median value of the different types of wetlands. **b** The shape index change of the different types of wetlands. **c** The surface temperature range and median value of the different types of wetlands

3.4 The temporal change of cooling effect

Based on our daily datum records of wetland cooling effects, the cooling effects of the Niuxintaobao marsh and the Zhangjialu Lake both persisted for 10 h (Fig. 8). However, the cooling effects of the Zhangjialu Lake started 3 h earlier than that of the Niuxintaobao Marsh, with starting-time of 5 a.m. and 8 a.m., respectively. The maximum cooling effects for the Niuxintaobao Marsh and the Zhangjialu Lake occurred at 2:45 p.m. and 0:45 p.m., respectively.

4 Discussion

4.1 The factors affecting cooling effect

4.1.1 Natural characteristics

We assessed the spatial extent and intensity of cooling effects for different types of wetland and their important characteristics that affect the cooling effects. The size and shaped complexity were important characteristics to determine wetland cooling effects. The western part of Jilin province belongs to Songnen Plain, with altitude from 120 to 200 m and ground slope is about 1/7000. The water depth in wetland was mostly between 0.4 and 1.5 m, except for a few large lake, especially significant positive correlation with the area of wetland, the correlation coefficient was 0.937 for lake, 0.858 for marsh, and 0.911for MLM, respectively ($p < 0.01$). So the size of wetland may indicate the water and heat capacity. However, in this study, there is no significant correlation in LSI index, cooling distance, and temperature difference (Fig. 9). From the curves, the temperature difference decreased with the increase of LSI index for all types of wetland. On the contrary, the cooling distance of lake, MLM, and marsh slowly increased with LSI value (Fig. 9). The phenomenon was not because the cooling distance increased with the wetland LSI value increase, but the area expansion of wetland led it.

In the western part of Jilin province, most precipitation concentrated in July and August and formed a lot of seasonal wetland with small area (Wang et al. 2008; Shen et al. 2014).

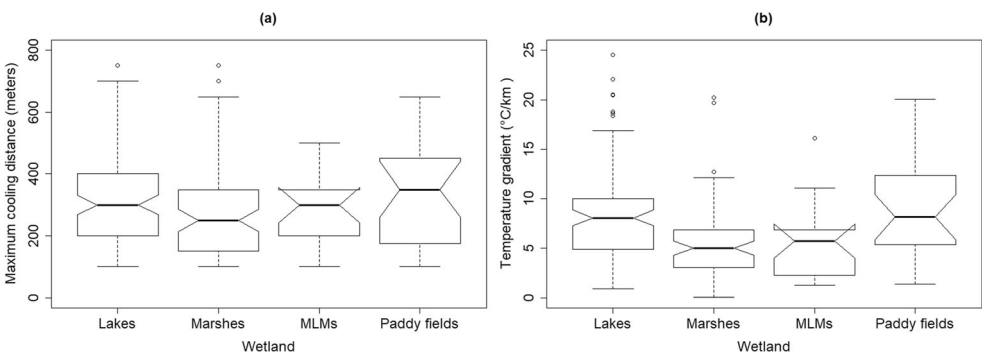

Fig. 5 The cooling effect of the different types of wetlands in the west of Jinlin province. **a** The maximum cooling affect range and median value of the different types of wetlands. **b** The temperature gradient range and median value of the different types of wetlands

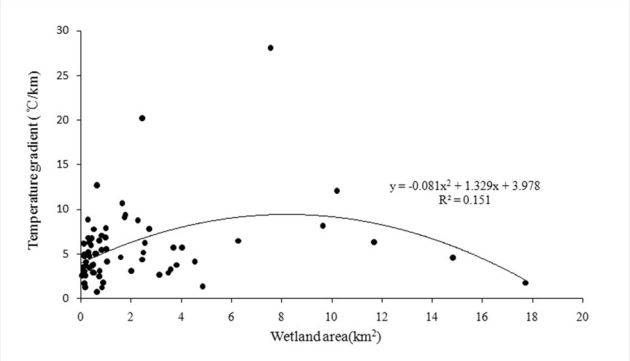

Fig. 6 The temperature gradient of marsh with different area

From Fig. 7, most wetlands (except artificial wetland) with an area of less than 2 km^2 showed almost similar amount of cooling effects with the larger ones. It suggested that though larger size of wetlands might have higher intensity and spatial extent of cooling effects, the small size wetlands cannot be neglected especially in semi-arid area.

4.1.2 Human disturbance and land use

It is known that changes are observed on microclimate depending on the effects of land use on energy exchange between the land surface and atmosphere and biogeochemical cycle and the ecosystem structure (Wang et al. 2017).In comparison with other land cover types, water bodies can store more heat and decelerate temperature variation; thus, wetlands can regulate the surrounding climate (Zhang et al. 2016; Çağdaş and Halime 2018). In this study, we found that paddy fields had the largest cooling effects than lakes followed by marshes and MLM. There are two main reasons for this phenomenon. The first reason is that the paddy field was mostly distributed on both sides of river, the fluidity of rivers could take away a lot of heat energy (Zhenshan et al. 2019). Western Jilin belongs to arid and semi-arid region in climate. The average annual rainfall is 400–500 mm and the average annual evaporation intensity is 1500–2000 mm (Zhao 2012). Most paddy fields in Western Jilin were irrigated with groundwater in which the temperature was about zero (Lu et al. 2013), so the groundwater needs a lot of heat energy to raise its temperature for irrigation.

The correlation coefficient in cooling effect, area, and LSI in rural area was not very high as previous studies in cities (Ranhao et al. 2012). The reason which leads to this phenomenon mostly was the complexity of different land use. In studies undertaken in cities, the water body (lake, pond, or wetland) were mostly surrounded by homogeneity building with roughly same brightness temperature and land surface emissivity for LST calculation (Ranhao et al. 2012; Zhang et al. 2016; Wang et al. 2017; Zhenshan et al. 2019). But in the rural area, the wetland was surrounded by different land use including farmland, forest, building, or bare land. Different land use with different brightness temperature and land surface emissivity would cause different LST value and lead to a little deviation of cooling effect (Zhang et al. 2014; Çağdaş and Halime 2018).

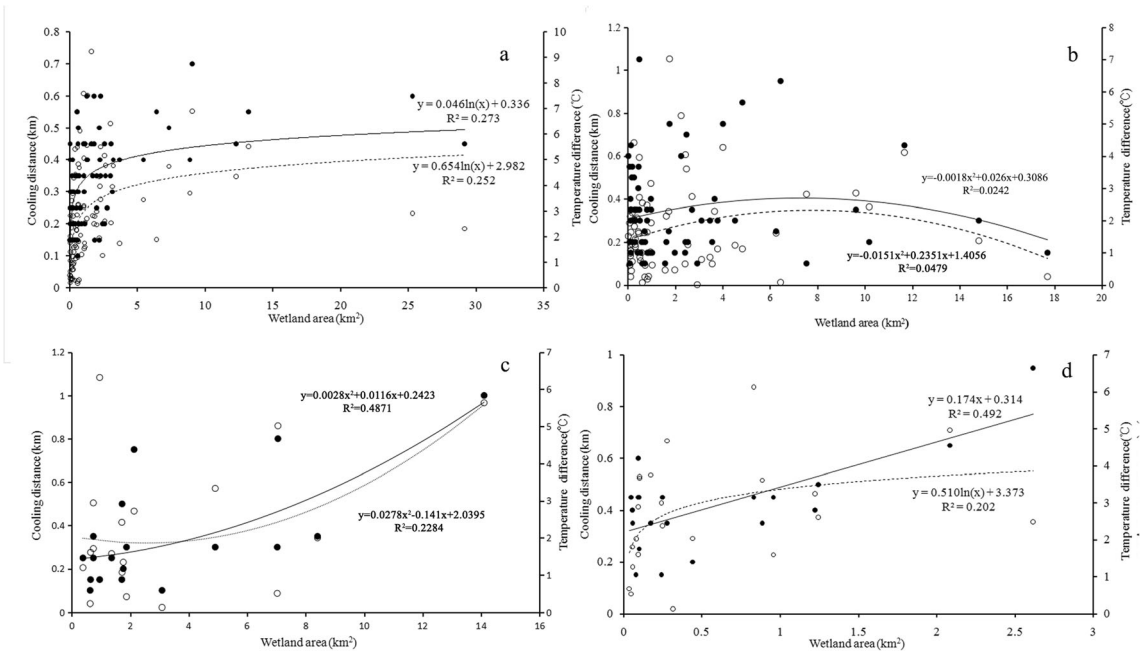

Fig. 7 The cooling effect of the different types of wetlands in the west of Jinlin province. Black dots represent cooling distance, black lines represent the variation trend, and Hollow point represent temperature difference, dashed lines indicate the trend of change.(**a**, **b**, **c**, **d** represent lake, marsh, MLM, and artificial wetland)

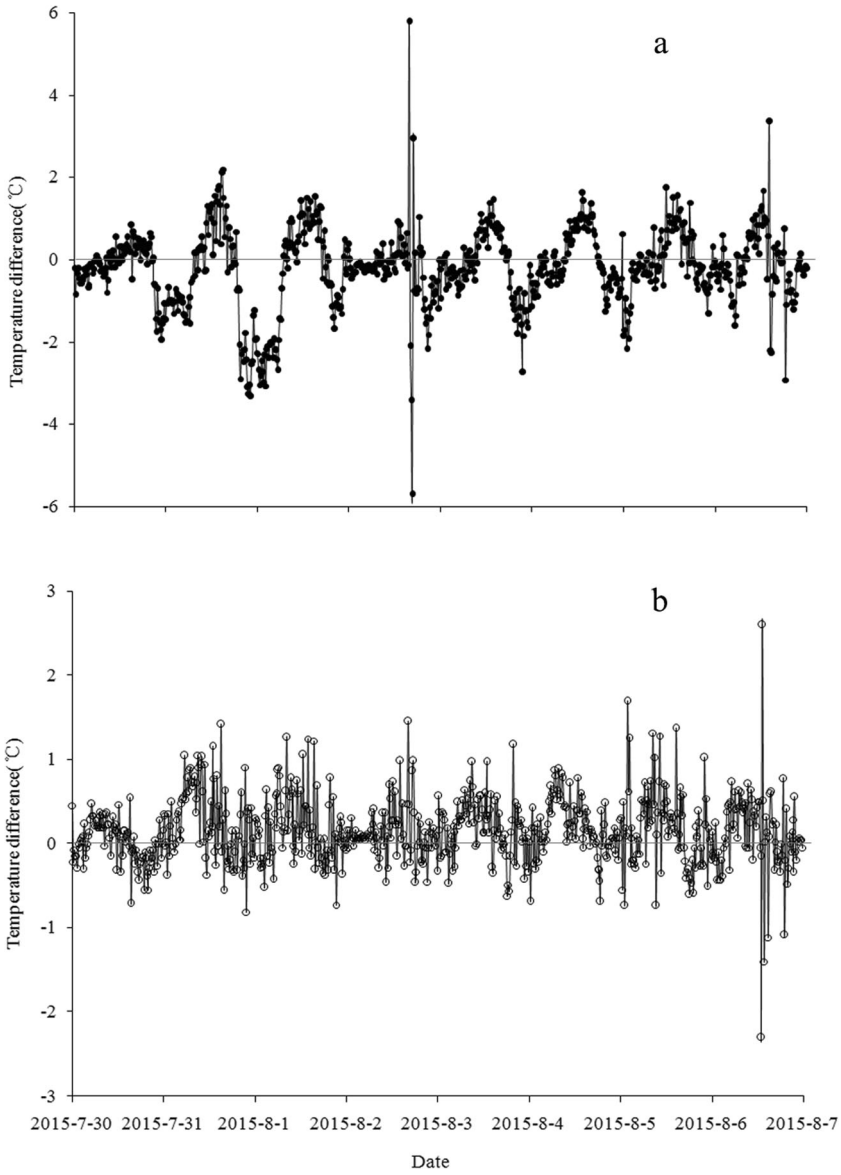

Fig. 8 The temperature difference between interior and outside wetland in marsh (**a**) and lake (**b**)

4.2 Implications for ecological function evaluation

Wetland function can be divided into three categories: hydrological function, biogeochemical function, and ecological function (Chen and Lu 2003). A lot of studies had evaluated the wetland ecological function from global change, water quality purification, and biodiversity maintenance (Fu and Li 2001; Zhifeng et al. 2013; Cristian et al. 2019). However, the evaluated methods maybe had ignored the wetland attributes, especially in large scale, such as vegetation proportion and soil characteristics. Two main findings in this study may provide some implications on the assessment of ecological functions. First, the case study of wetland landscape in west Jilin province showed that the cooling effect was obvious during the daytime with different spatial and temporal variations. This indicated that cooling effects of wetlands should be included and calculated in the evaluation of wetland ecological functions. Second, the characteristics of different wetland types and spatial interactions between wetland landscape play an important role in ecological function, particularly in hydrological pathways, soil fertility, and biodiversity (Bennett et al. 2009; Drexler et al. 2009; Gordon et al. 2008).

From the research, we found that the wetlands with small area less than 2 km^2 were disorderly scattered in the semi-arid area surrounded by uplands. The isolated wetlands maybe had episodic or slow hydrological and biogeochemical connectivity, but this condition does not imply the absence of hydrological, biogeochemical, and biological exchanges with nearby wetlands (Cohen et al. 2016), especially in biodiversity support. The west of Jilin Province is an important distribution area of bird habitat.

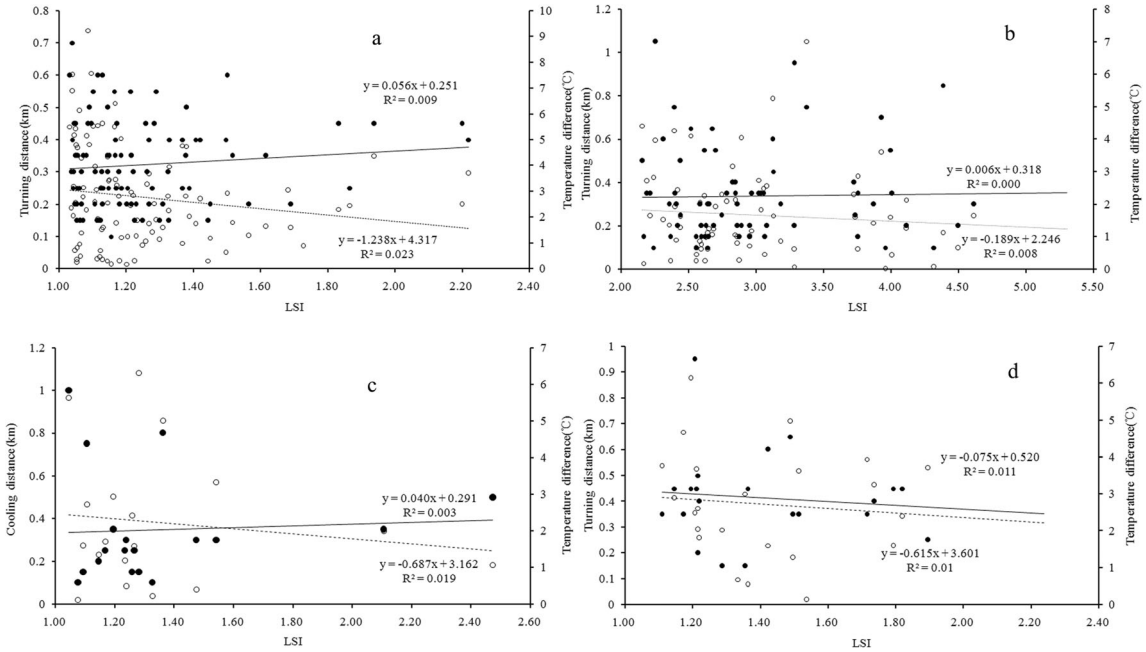

Fig. 9 The LSI index of the different types of wetlands in the west of Jinlin province. Black dots represent turning distance, black lines represent the variation trend, hollow points represent temperature difference, and dashed lines indicate the trend of change. **a**, **b**, **c**, and **d** represent lake, marsh, LMM, and artificial wetland

There are several wetlands that are on the list of wetlands of international importance, such as the Momoge wetland and Xianghai wetland. Thousands of birds migrate and breed in this region including many rare or threatened species (Yang et al. 2006). But in the evaluation of ecological function, some isolated wetlands maybe neglected for lack of monitoring data.

4.3 Implication for local climate change

With strong evapotranspiration and huge heat storage characteristics, wetlands play an important role in climate regulation for their own radiation and thermal and water properties (Carrington et al. 2001; Nakayama and Fujita 2010; Bai et al. 2013; Gou et al. 2014). In radiation amount, the latent heat flux of wetland is generally more than sensible heat flux about 50% (Liu et al. 2015). The results of previous studies indicated that cooling effect of wetlands are closely related to factors such as season, wetland area, and LSI index (Gerhard 2003; Zhang et al. 2004). In this study, we found that different wetland types have different cooling effects and mechanisms. The wetland influence on microclimate could not be simply lumped together for different water evaporation and plant transpiration. In this study, the cooling effect of lake was 3 h ahead of marsh (Fig.8), and it showed that the different types of wetland temperature reach equilibrium point in different time, and the cooling effect in daytime was mainly affected by the heat capacity and dissipation rate. Meanwhile, the isolated wetland with small area showed relatively further turning distance and temperature difference; it implied that firstly the wetland was less affected by adjacent wetlands and secondly it was distributed in further arid areas. We sought to determine whether there is the characteristics threshold for regulating microclimate of wetland, such as area or vegetation proportion, below which the ecological function is negligible. But now, more in-depth researches were needed.

5 Conclusions

We assessed the cooling effects of different wetland types in a semi-arid region, Northeast China using Landsat 8 images. The results showed that paddy fields had the largest cooling effects followed by lakes, marshes, and MLMs. The cooling effects generally increased with increases in wetland area while it decreased with the shape complexity. Small size wetlands may have large cooling effects compared with the large ones. Our study provided useful implications for the assessment of ecosystem services and quantifying the microclimate regulation services, especially in designing optimization of regional land use pattern.

Acknowledgments We thank the editor and anonymous referees for their precious time.

Funding information The study was supported by the National Science Foundation of China (NSFC41371193, NSFC41101091, and NSFC41471080).

References

Bai J, Lu Q, Zhao Q, Wang J, Ouyang H (2013) Effects of alpine wetland landscapes on regional climate on the Zoige plateau of China. Adv Meteorol 10(1):1–7

Bennett EM, Peterson GD, Gordon LJ (2009) Understanding relationships among multiple ecosystem services. Ecol Lett 12:1394–1404

Burkett V, Kulser J (2000) Climate change: potential impacts and interactions in wetlands of the United States. J Am Water Resour Assoc 36(2):313–320

Çağdaş KŞ, Halime Ö (2018) Investigation of the effects of wetlands on micro-climate. Appl Geogr 97:48–60

Carrington DP, Gallimore RG, Kutzbach JE (2001) Climate sensitivity to wetlands and wetland vegetation in mid-Holocene North Africa. Clim Dyn 17:151–157

Chen CQ, Lei CX, Wang CC, et al (2011) Changes of spring maize potential productivity under the background of global warming in Northeast China. Scientia Geograph Sinica 31(10):1272–1279

Chen Y, Lu X (2003) The wetland function and research tendency of wetland science. Wetland Sci 1(1):7–10 (in Chinese)

Cohen JM, Irena FC, Laurie A et al (2016) Do geographically isolated wetlands influence landscape functions? PANS 113(8):1979–1986

Costanza R, d'Arge R, de Groot RS et al (1997) The value of the world's ecosystem services and natural capital. Nature 387:253–260

Costanza R, D'Arge R, de Groot R et al (1998) The value of the world's ecosystem services and natural capital. Ecol Econ 25:3–15

Cristian F-O, Escaff D, Cisternas J (2019) Spiral vegetation patterns in high-altitude wetlands. *Ecol Complex* 37:38–46

Dash P, GãTtsche FM, Olesen FS, Fischer H (2002) Land surface temperature and emissivity estimation from passive sensor data: theory and practice-current trends. Int J Remote Sens 23(13):2563–2594

Davidson NC (2014) How much wetland has the world lost? Long-term and recent trends in global wetland area. Mar Freshw Res 65:936–941

Drexler JZ, Fontaine CS, DeDeverel et al (2009) The legacy of wetland drainage on the remaining peat in the Sacramento-San Joaquin Delta, California, USA. Wetland 29:372–386

Du H, Song X, Jiang H et al (2016) Research on the cooling island effects of water body: a case study of Shanghai, China. Ecol Indic 67:31–38

Du C, Ren H, Qin Q, Meng J, Zhao S (2015) A practical split-window algorithm for estimating land surface temperature from Landsat 8 data. *Remote Sens* 7(1):647–665

Fu G, Li K (2001) Progress in the study on the relationship between global warming and wetland ecological system. Geogr Res 20(1):120–128 (in Chinese)

Gao J, Lu X, Li Zhao F (2002) Study on cold-humid effect of wetlands in Sanjiang plain. J Soil Water Conserv 16(4):149–151 (in Chinese)

Gao J, Lu X, Hongyu L (2003) Cold-humid effect of wetlands. J Ecol Rural Environ 19(1):18–21 (in Chinese)

Gerhard K (2003) Impact of lakes and wetlands on boreal climate. J Geophys Res 108(16):1–17

Gong X, Wang Y, Xiao N et al (2011) Differences in air temperature and relative humidity between a marsh wetland and its surrounding dry farmland. J Northeast Forest Univ 39(11):93–96 101. (in Chinese)

Gordon BB (1995) Sensitivity of a GCM simulation to inclusion of inland water surface. J Clim 8(1):2691–2704

Gordon LJ, Peterson GD, Bennett EM (2008) Agricultural modifications of hydrological flows create ecological surprises. Trends Ecol Evol 23:211–219

Gou QQ, Qu JJ, Han ZW (2014) Microclimate and CO2 fluxes on continuous fine days in the Xihu desert wetland, China. J Arid Land 7(3):318–327

Hostetler SW, Bates GT, Giorgi F (1993) Interactive coupling of a lake thermal model with a regional climate model. J Geophys Res-Atmos 98(3):5045–5057

Lahmer W, Pfuetnner B, Becher A (2001) Assessment of land use and climate change impacts on the mesoscale. Phys Chemist Earth B 26(7–8):565–575

Li F, Zhang S, Yang J, et al (2016) The effects of population density changes on ecosystem services value: a case study in Western Jilin, China. Ecol Indic 61:328–337

Li F, Zhang S, Yang J et al (2018) Effects of land use change on ecosystem services value in West Jilin since the reform and opening of China. Ecosyst Serv 31:12–20

Li ZL, Wu H, Wang N, Qiu S, Wan Z, Tang BH, Yan G (2013) Land surface emissivity retrieval from satellite data. Int J Remote Sens 34(9-10):3084–3127

Liu Y, Sheng L, Liu J (2015) Impact of wetland change on local climate in semi-arid zone of Northeast China. Chin Geogr Sci 25(3):309–320

Lu WX, Chen SM, Luo JN (2013) Meteorological drought characteristics research of Western Jilin Province based on wavelet analyses. Appl Mech Mater 295-298:2121–2126

Mingquan W, Wang J, Liu J (2008) Analysis of the coupling between resource-environment and population economy in West Jilin Province. Bull Soil Water Conserv 28(2):167–172 (in Chinese)

Mitsch WJ, Gosselink JG (2007) Wetlands, 4th edn. John Wiley & Sons Inc, New York, USA, pp 85–100

Nakayama T, Fujita T (2010) Cooling effect of water-holding pavements made of new materials on water and heat budgets in urban areas. Landsc Urban Plan 96:57–67

Nie X, Wang Y (2010) "Cold-humidity island" effect of marsh wetlands on localized micro-climate. J Ecol Rural Environ 26(2):189–192 (in Chinese)

Offer R, Qin Z, Derimian Y, Karnieli A (2014) Derivation of land surface temperature for Landsat-8 TIRS using a split window algorithm. *Sensors* 14(4):5768

Qin ZH, Karnieli A, Berliner P (2001a) A mono-window algorithm for retrieving land surface temperature from Landsat TM data and its application to the Israel-Egypt border region. Int J Remote Sens 22(18):3719–3746

Qin Z (2005) A practical split-window algorithm for retrieving land-surface temperature from MODIS data. Int J Remote Sens 26(15):3181–3204

Qin Z, Gao M (2006) An algorithm to retrieve land surface temperature from ASTER thermal band data for agricultural drought monitoring. Proceedings of SPIE - The International Society for Optical Engineering 6359:32

Qin Z, Dall'Olmo G, Karnieli A, Berliner P (2001b) Derivation of split window algorithm and its sensitivity analysis for retrieving land surface temperature from NOAA-advanced very high resolution radiometer data. J Geophys Res-Atmos 106(D19):22655–22670

Ramsar Convention on Wetlands, 2014. Information sheet on Ramsar wetlands. BanrockStation Wetland Complex (). https://rsis.ramsar.org/RISapp/files/RISrep/AU1221RIS_1405_en.pdf

Ramsar Convention on Wetlands, FAO, International Water Management Institute, 2014.Wetlands and agriculture: partners for growth. (). http://www.ramsar.org/sites/default/files/wwd14_leaflet_en.pdf

Ranhao S, Chen A, Chen L (2012) Cooling effects of wetlands in an urban region: the case of Beijing. Ecol Indic 20:57–64

Shen XJ, Wu ZF, Du HB (2014) Characteristics of climatic change in semiarid region of western Jilin in recent 50a. J Arid Land Resour Environ 28(2):190–196 (in Chinese)

Snyder WC, Wan Z, Zhang Y, Feng YZ (1998) Classification-based emissivity for land surface temperature measurement from space. Int J Remote Sens 19(14):2753–2774

Turner RK, Jeroen CJM, Bergh V et al (2000) Ecological-economic analysis of wetlands scientific integration for management and policy. Ecol Econ 35(1):7–23

Wang H, Zhang Y, Tsou JY, et al (2017) Surface urban heat island analysis of Shanghai (China) based on the change of land use and land cover. Sustainability 9(9):1538

Wang M, Wang J, Liu J (2008) Analysis of the coupling between resource-environment and population economy in West Jilin Province. J Soil Water Conserv 28(2):167–172 (in Chinese)

Yang B, Yu G, Xiaowei S et al (2006) The avifauna of Momoge nature reserve in Jilin Province. Chin J Zool 41(6):82–91

Yu Y, Privette JL, Pinheiro AC (2007) Evaluation of split-window land surface temperature algorithms for generating climate data records. IEEE Transac Geosci Remote Sens 46(1):179–192

Zhang, W., Jiang, J., Zhu, Y. 2014. Change in urban wetlands and their cold island effects in response to rapid urbanization. Chinese Geographical Science. https://doi.org/10.1007/s11769-015-0764-z

Zhang W, Zhu Y, Jiang J (2016) Effect of the urbanization of wetlands on microclimate: a case study of Xixi wetland, Hangzhou, China. Sustainability 8:885

Zhang Y, Lyu X, Ni J (2004) Cold-humid ecological effects of the Sanjiang Plain. Ecol Environ13 (1):37–39 (in Chinese)

Zhao H (2012) Study on the ecological water level and water volume regulation of groundwater in west plain area of Jilin Province. China University of Geosciences, Beijing, pp 4–18 (in Chinese)

Zhenshan X, Guanglei H, Zhongsheng Z, Xianguo L, Ming J, Yuanchun Z, Xiangjin S, Jie W, Xiaohui L (2019) Quantifying the cooling-effects of urban and peri-urban wetlands using remote sensing data: case study of cities of Northeast China. Landsc Urban Plan 182:92–100

Zhifeng Y, Qin Y, Yang W (2013) Assessing and classifying plant-related ecological risk under water management scenarios in China's Yellow River Delta wetlands. J Environ Manag 130: 276–287